



Heat Transfer and Pressure Drop Characteristics of Nanofluids in a Plate Heat Exchanger

Y. H. Kwon¹, D. Kim¹, C. G. Li¹, J. K. Lee¹, D. S. Hong²,
J. G. Lee², S. H. Lee³, Y. H. Cho³, and S. H. Kim^{4,*}

¹School of Mechanical Engineering, Pusan National University, 609-735, Republic of Korea

²Institute of Samchang Tsinghua Nano Application, N-BARO TECH, 689-871, Republic of Korea

³Air Conditioning Energy Company, LG Electronics, Republic of Korea

⁴College of Nanoscience and Nanotechnology, Pusan National University, 609-735, Republic of Korea

In this paper, the heat transfer characteristics and pressure drop of the ZnO and Al₂O₃ nanofluids in a plate heat exchanger were studied. The experimental conditions were 100–500 Reynolds number and the respective volumetric flow rates. The working temperature of the heat exchanger was within 20–40 °C. The measured thermophysical properties, such as thermal conductivity and kinematic viscosity, were applied to the calculation of the convective heat transfer coefficient of the plate heat exchanger employing the ZnO and Al₂O₃ nanofluids made through a two-step method. According to the Reynolds number, the overall heat transfer coefficient for 6 vol% Al₂O₃ increased to 30% because at the given viscosity and density of the nanofluids, they did not have the same flow rates. At a given volumetric flow rate, however, the performance did not improve. After the nanofluids were placed in the plate heat exchanger, the experimental results pertaining to nanofluid efficiency seemed inauspicious.

Keywords: Nanofluids, Heat Transfer Coefficient, Thermal Conductivity, Plate Heat Exchanger.

1. INTRODUCTION

When applying nano-sized particles to fluids in a dispersed way, the fact that a large portion of such problems as sedimentation in the heat exchanger tube, increase in pressure drop, and wear of the pump and moving parts can be overcome by the formation of a nanoparticle-sized fluid with excellent dispersion stability was reported in preliminary researches,¹ and there is a high possibility of heat transfer fluid application. Heat transfer is the transfer of heat energy moving due to temperature difference, or the energy caused by irregular particle movement or thermal diffusion. Hence, the studies on such heat transfer fluids have focused on the development of a fluid with high heat conductivity and thermal diffusivity, and a large portion of the research has been on the development of the correlation of the convection heat transfer coefficient with the increment of heat conductivity.² Due, to the fact, however, that many relevant theories have been gathered, the results of the measurement of heat conductivity differ in the heat conductivity elevation experiments according to the type of nanofluid particles used and

the increment percentage, making quantitative comparison analysis impossible. Buongiorno et al.³ recently carried out a research in which many scholars studying nanofluids made the same nanofluid, measured its heat conductivity, and reported the result.

Kang⁴ reported that in the study he conducted, the overall heat transfer coefficient increased by 12.5% compared to the insulating oil when 0.5 vol% γ -Al₂O₃ (40 nm) was measured from the 100 to 400 Reynolds numbers, using insulating oil type 1 no. 4 and oleic and lauric acid as dispersing agents. Choi⁵ proved the result in which the overall heat transfer coefficient increased by a maximum of 20% in the case of the globular- and plane-shaped particles of 0.5 vol% Al₂O₃ (13.2 × 20, 200 nm) and the globular-shaped particles of 0.5 vol% AlN, as a result of the application of plate heat transfer using the divisions of bead milling and ultrasonic bath, and oleic acid as a dispersing agent. Moreover, Pantzali⁶ reported that the efficiency of heat conductivity according to the increment of volume flow manifests an insignificant increase compared to water, whereas the pumping power increases by 40~50% compared to water under the same heat exchange rate condition, as the result of the application of 4.0 vol% CuO (30 nm) using a CTAB dispersing agent on a plate

* Author to whom correspondence should be addressed.

heat exchanger and analyzing the heat flux (Q) according to the increment of the Reynolds number as well as the heat flux (Q) according to the increment of volume flow and pumping power (W). It was also judged that viscosity increment restrains the effect of warm current and convection heat transfer, as the characteristics of the plate heat exchanger's electric plate, by analyzing the flow characteristics of the fluid inside the electric plate via CFD. This was confirmed by the more than 20% increase in heat conductivity efficiency when the same heat exchange fluid (4 vol% CuO) was applied on the plane plate heat exchanger rather than on the plate heat exchanger.

Above all, the purpose of this paper was to measure the basic thermophysical properties then to apply plate heat transfer that is easy to disassemble or assemble, where the addition or subtraction of a plate will make it possible to make a decision regarding the sedimentation in the heat exchanger tube, and to evaluate the heat transfer coefficient and pressure drop characteristics. Finally, this study is expected to help prove the possibility of nanofluid application.

2. EXPERIMENTAL DETAILS

2.1. Preparation of Nanofluids

In a preliminary study, the particles with superior thermal conductivity were analyzed. Al_2O_3 , CuO, TiO_2 , and ZnO in oxide, Ag in metal, and CNT and graphite in the carbon group were chosen as particles for the experiment. Although CuO has generally better thermal conductivity and particle dispersion, it was impossible to use CuO due to its absorption problem. Compared to CuO, the thermal conductivity and particle dispersion of TiO_2 are inferior. Moreover, Ag revealed problems, such as in relation to absorption and oxidation. CNT and graphite showed better thermal conductivity but demonstrated dispersion stability weakness. Al_2O_3 and ZnO were thus chosen for use in this paper as they have superior thermal conductivity and dispersion stability despite their low prices. The transmission electron microscopy (TEM) image of Al_2O_3 is shown in Figure 1, where it can be seen that the nanoparticles were spherical and had 20~50 nm sizes. Figure 2 shows ZnO with stick form particles 20~60 nm in size.

2.2. Measurement of the Thermophysical Properties

The results of the measurement of the basic thermophysical properties of the Al_2O_3 and ZnO nanofluids, such as thermal conductivity, using the transient hot-wire method, are shown in Figure 3. The thermal-conductivity results were 4.1, 7.3, and 11% for the 1, 3, and 6 vol% Al_2O_3 . Moreover, the value increased to 5.2% for the 1 vol% ZnO. The kinematic-viscosity results shown in Figure 4, which were obtained using an Ubbelohde viscometer, went up to 65% in Al_2O_3 and to 7.6% in ZnO. In addition, the results

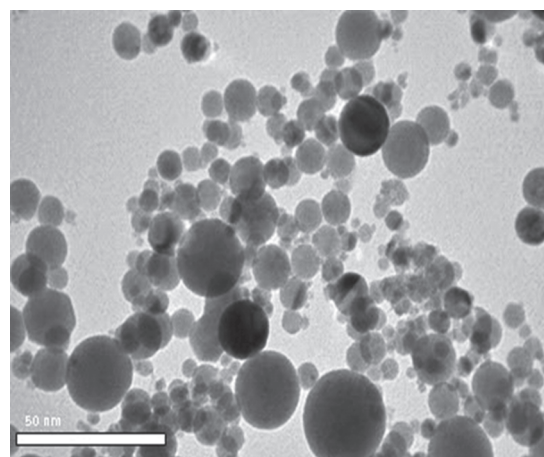


Fig. 1. TEM image of the aluminium oxide nanoparticles dispersed in nanofluids.

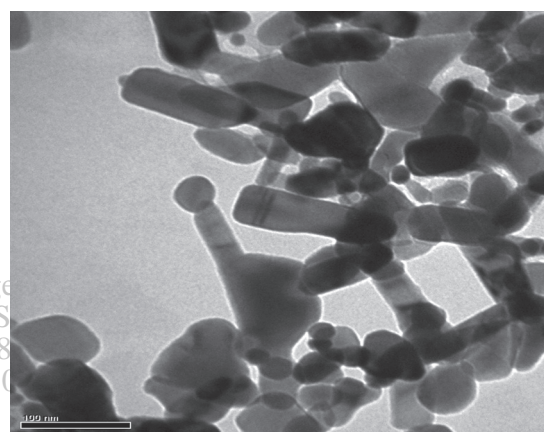


Fig. 2. TEM image of the zinc oxide nanoparticles dispersed in nanofluids.

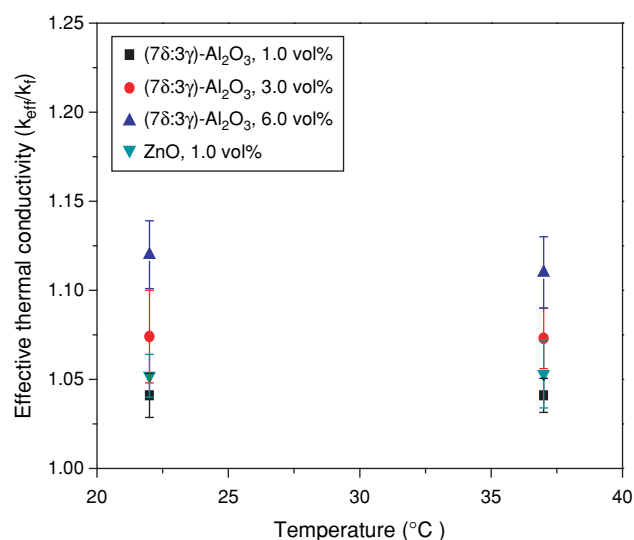


Fig. 3. Thermal conductivity of the nanofluids.

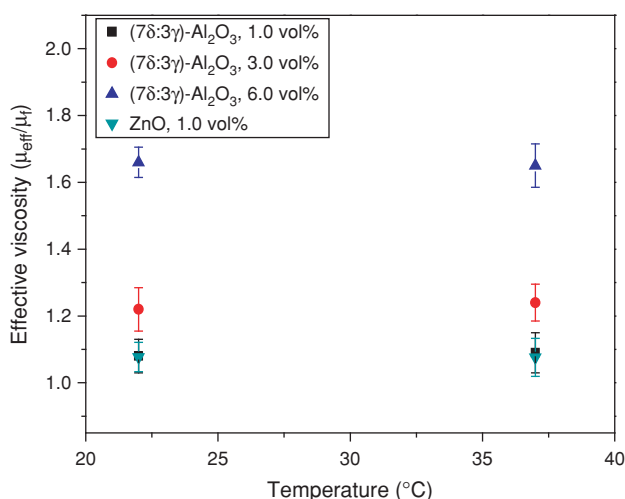


Fig. 4. Kinematic viscosity of the nanofluids.

of the measurement of the zeta potentials for the examination of the dispersion stability were excellent: 50.84 mV (pH = 4.3) in Al_2O_3 , and -44.0 mV (pH = 12.5) in ZnO. After one week, no sedimentation effect occurred.

3. EXPERIMENTAL SETUP

Figure 5 shows a schematic diagram of the plate heat exchanger that was used in this study, which was an SUS316 fluid gasket with a 1.5 kW maximum heat exchange rate, composed of seven sheets. Figure 6 shows the structure of the used plate. The detailed specifications are shown in Table I. The heat exchange experimental device is composed of high- and low-temperature flowing paths. The temperature of the heat exchanger is kept at 40 ± 0.5 °C upon the entry of high-temperature side fluid, and at 20 ± 0.5 °C upon the entry of low-temperature side fluid. A pre-heater is installed on the high-temperature

side, and a chiller on the low-temperature side, to maintain a certain temperature. To analyze the heat exchanger's thermal performance and pressure loss, a T -type thermocouple was installed inside the pipes at the high- and low-temperature entry sides to measure the temperatures, and the pressure loss was measured by attaching a seizer to each layer. The fluid flux of the experimental device was $0.8 \sim 2.4$ kg/m in the method involving the adjustment of the valve and pump-applied voltage. The flux was measured using a mass flow meter, and the range of the Reynolds number of the heat exchanger was 100–500. In the case of the general plate heat exchanger, it generates a warm-current effect in the domain of a low Reynolds number, and it is known to show the characteristics of turbulent flow at the 100 Reynolds number and over, according to a reference. Hence, this study was conducted specifically to experiment on the Reynolds number up to the maximum of 500, considering the pump discharge rate and the size of the experimental pipe gauge.

4. RESULTS AND DISCUSSION

The heat transfer in the plate heat exchanger of the hot and cold stream was shown as having used correlation (1) and (2), and the error correlation with the heat rate was shown as correlation (3). Heat transfer was conducted within a 5% error range, and the experiment results are the same as those shown in Figure 7. In particular, this study used the correction of the preliminary empirical correlation (Wanniarachichi, 1995), and the results were within a 5% error range, as shown in Figure 8.

$$Q_h = \dot{m}_h c_{p,h} (T_{h,i} - T_{h,o}) \quad (1)$$

$$Q_c = \dot{m}_c c_{p,c} (T_{c,o} - T_{c,i}) \quad (2)$$

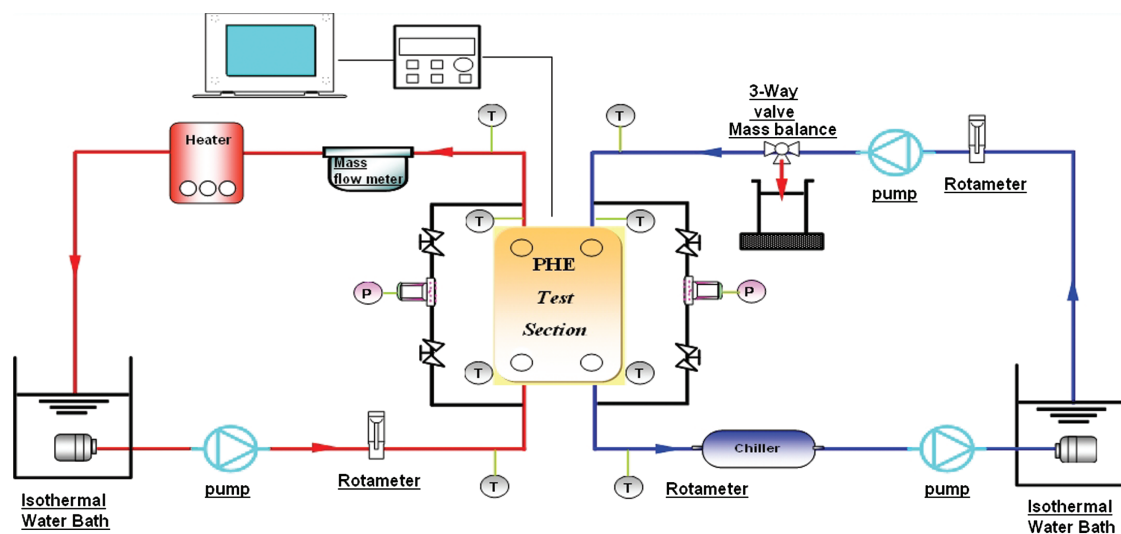


Fig. 5. Schematic diagram of the experimental apparatus.

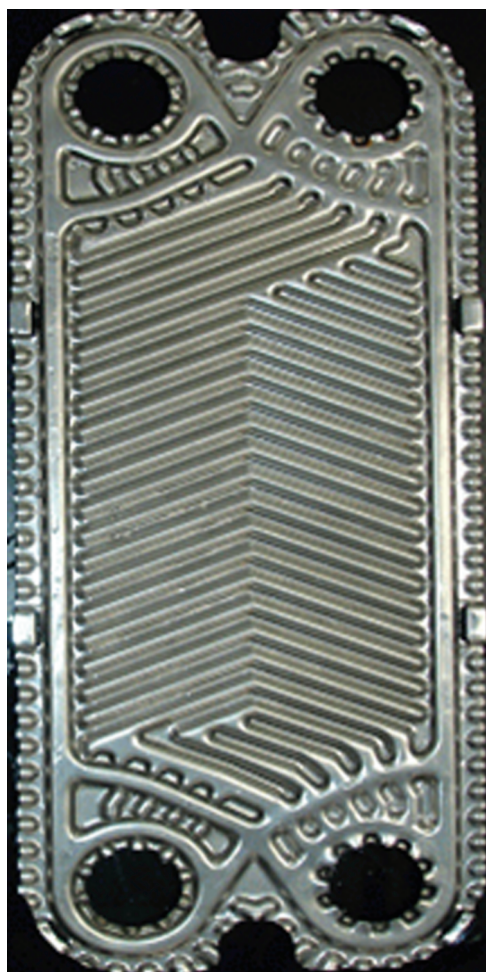


Fig. 6. Photograph of the plate heat exchanger.

$$\text{Error}(\%) = \left| \frac{Q_h - Q_c}{Q_h} \right| \times 100 \quad (3)$$

In the above equations, m is the mass flow rate of the basic fluids, c is the effective specific heat, and T is the inlet and outlet temperature. After measuring the temperature in the inlet and outlet, the use of LMTD for investigating the heat transfer characteristic in the heat exchanger was expressed in the following correlation:

$$\Delta T_{\text{LMTD}} = \frac{(T_{h,i} - T_{c,o}) - (T_{h,o} - T_{c,i})}{\ln(T_{h,i} - T_{c,o} / T_{h,o} - T_{c,i})} \quad (4)$$

Table I. Geometric characteristics of the plate heat exchanger.

Vertical port distance, L_v (m)	0.2
Horizontal port distance, L_h (m)	0.05
Effective channel width, L_w (m)	0.075
Corrugation amplitude, b (m)	0.0018
Port diameter, D_p (m)	0.0275
Chevron angle	30°
Heat transfer area (m^2)	0.076
Number of plates	7

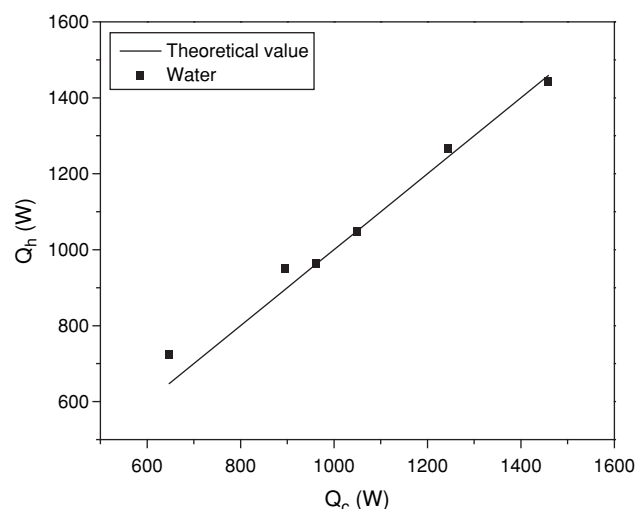


Fig. 7. Heat balance of the plate heat exchanger for water.

Correlation (5) is the result of the heat flow rate when LMTD was used as a plate heat exchanger. As the overall heat transfer coefficient, the sum of the convective heat resistance in the hot and cold stream and the conduction

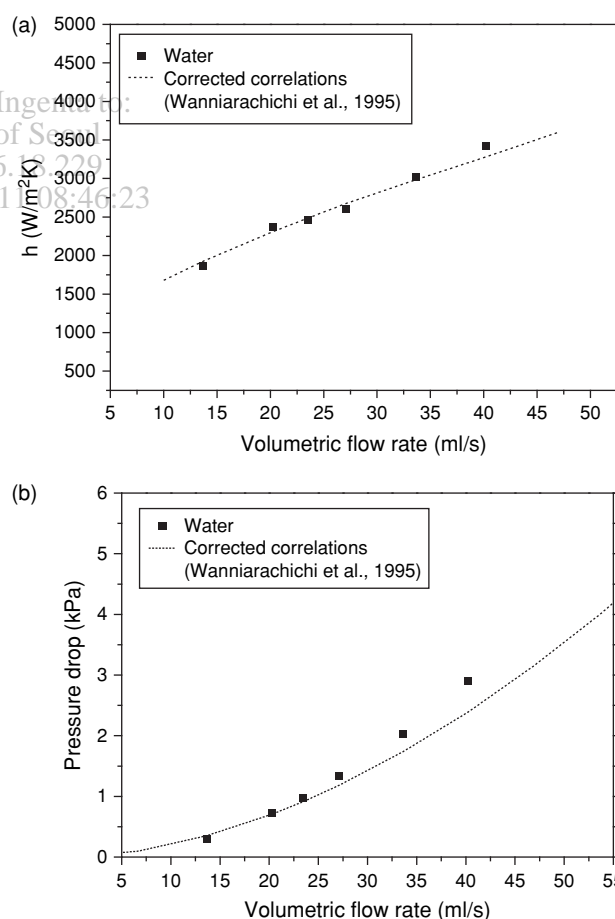


Fig. 8. Comparison of the results of the measurement with the corrected empirical Wanniarachichi equation of water for (a) convective heat transfer rate and (b) pressure drop.

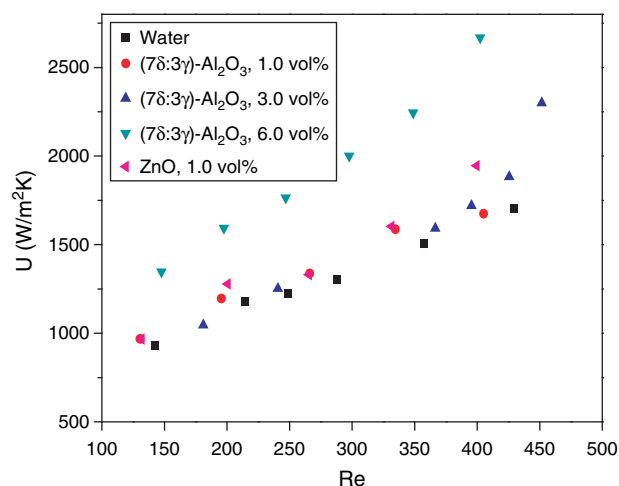


Fig. 9. Overall heat transfer coefficient as a function of Reynolds number.

resistance of the heating place in the heat exchanger was shown as correlation (6).

$$Q = UA\Delta T_{LMTD} \quad (5)$$

$$\frac{1}{U} = \frac{1}{h_c} + \frac{t}{k_s} + \frac{1}{h_h} \quad (6)$$

In the above equation, U is the overall heat transfer coefficient, k_s is the thermal conductivity of the plate, t is the thickness of the plate, h_c is the cold liquid, and h_h is the hot liquid. Figure 9 shows the overall heat transfer coefficient as a function of the Reynolds number. At the specific 400 Reynolds number, where 1, 3, and 6 vol% Al_2O_3 was applied, the result under 6 vol% Al_2O_3 increased to 30%. In the case of the 1 vol% ZnO, the overall heat transfer coefficient went up to approximately 14.5%. In the pressure drop in Figure 10, under the condition of 6 vol% Al_2O_3 , the pressure drop increased to

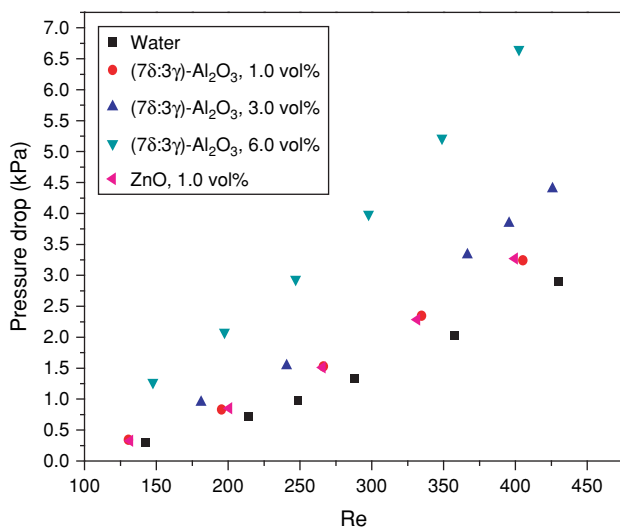


Fig. 10. Pressure drop as a function of Reynolds number.

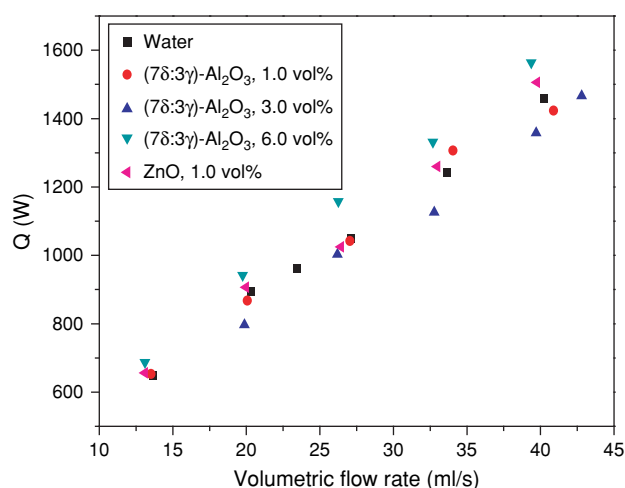


Fig. 11. Heat flow rate as a function of volumetric flow rate.

84.5%, and to 11.5% in the case of 1 vol% ZnO. Nevertheless, because the viscosity and density inside nanofluids are not same, the results of this experiment should not be examined based on the Reynolds number standards, when studying the heat transfer characteristics. This is why the flow rate in the heat exchanger goes up according to the increase in the nanofluid viscosity, compared to the general fluids. Therefore, this experiment should be evaluated based on the volumetric flow rate, considering the viscosity and density, when examining the heat exchanger efficiency. The purpose of studying the heat exchanger efficiency was summarized in Figure 11 as being related to the volumetric flow rate. The results were the following. The heat flow rate did not increase under 1 and 3 vol% Al_2O_3 , but the figure went up to approximately 7% only in the case of the 6 vol% Al_2O_3 . In the case of 1 vol% ZnO, based on the volumetric flow rate, the figures were within the experimental errors. Therefore,

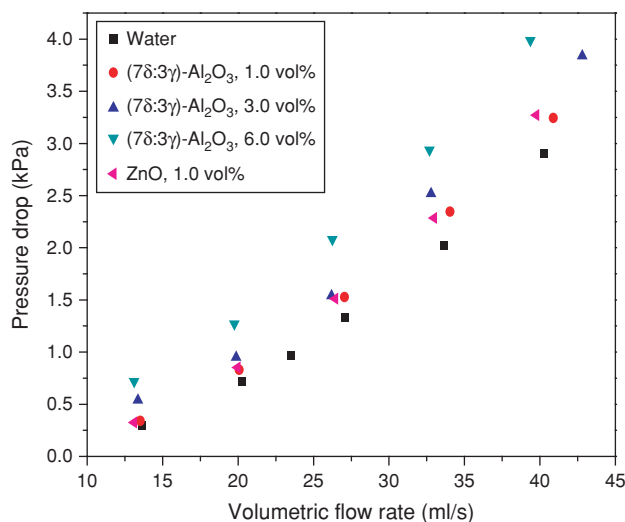


Fig. 12. Pressure drop as a function of volumetric flow rate.

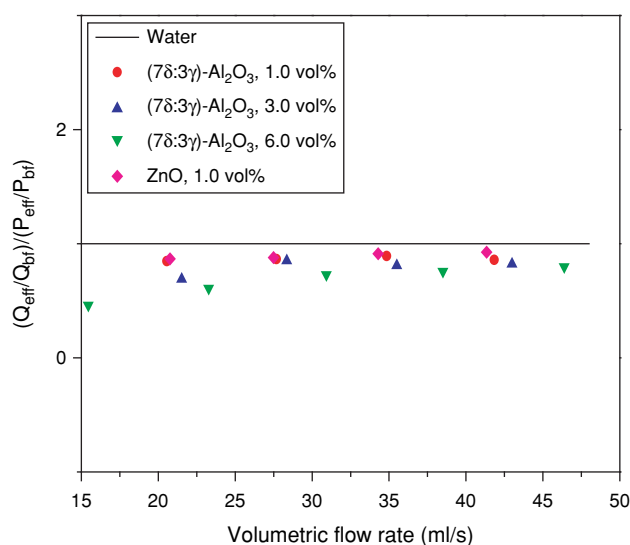


Fig. 13. Analysis of the efficiency of the nanofluids in a plate heat exchanger.

the experiment was performed only for the 1 vol% ZnO. Figure 12 shows the pressure drop results in the plate heat exchanger measurements, with the changes in the volumetric flow rate. As the volume of the nanofluids became higher, the pressure drop increased linearly. Under 6 vol% Al_2O_3 , the figure went up to 40%, as opposed to water.

In this paper, the nanofluid efficiency applied to the plate heat exchanger was studied by measuring the heat flow rate (W) and pumping power (W) according to the volumetric flow rate. The experiment, however, failed to conclusively prove the nanofluid efficiency, as in the final results shown in Figure 13. Pantzali et al.⁷ reported that this phenomenon is related to the plate structure, then concluded that an increase in viscosity suppresses the convective heat transfer coefficient, and an increase in thermal conductivity cannot make up for it when analyzing the fluid's moving characteristics in the plate. On the contrary, this study showed the most suitable condition of nanofluid existence through the experiment results. As such, the properties of nanofluids should be correctly defined, and the correspondence between thermal conductivity and viscosity should be investigated. Then the most proper nanofluids should be developed.

5. CONCLUSIONS

This study was performed by fabricating two-step Al_2O_3 and ZnO nanofluids, which have excellent dispersion stability. After measuring the thermophysical properties of such nanofluids, the obtained figures were applied to the plate heat exchanger for the measurement of the heat transfer coefficient and the pressure drop. The results were as follows:

- (1) The overall heat transfer coefficient according to the same Reynolds number increase went up to 30% under 6 vol% Al_2O_3 compared to water. As for the heat transfer efficiency with increasing volumetric flow rate, however, the heat transfer increase under 1 and 3 vol% Al_2O_3 was not high compared to that under water. The result went up to a maximum value of 7% only under 6 vol% Al_2O_3 .
- (2) When the pressure drop was analyzed in the same volumetric flow rate, the pressure drop increased linearly as the Al_2O_3 nanofluid volume went up. Moreover, the result rose to a maximum of 40% under 6 vol% Al_2O_3 .
- (3) This experiment failed to prove (by examining the nanofluid efficiency in the plate heat exchanger) the utmost effectiveness of nanofluid application according to the structural characteristics of the plate heat exchanger.

Acknowledgment: This work was supported by Grant No. 10026688 from the Advanced Technology Center Project of the Ministry of Knowledge Economy of the Republic of Korea.

References and Notes

1. W. Williams, J. Buongiorno, and L.-W. Hu, *Trans. ASME J. Heat Transfer* 130, 7 (2008).
2. S. U. S. Choi, Z. G. Zhang, W. Yu, F. E. Lockwood, and E. A. Grulke, *Appl. Phys. Lett.* 79, 2252 (2001).
3. J. Buongiorno, D. C. Venerus, and N. Prabhat et al., *J. Appl. Phys.* 106, 094312 (2009); A. Kido and Y. Lizumi, *Appl. Phys. Lett.* 73, 2721 (1998).
4. H. U. Kang, W. G. Kim, and S. H. Kim, *Theories and Applications of Chem. Eng.* 11 (2005).
5. C. Choi, H. S. Yoo, and J. M. Oh, *Current Applied Physics* 8, 710 (2008).
6. M. N. Pantzali, A. A. Mouza, and S. V. Paras, *Chem. Eng. Sci.* 64, 3290 (2009).
7. M. N. Pantzali, A. G. Kanaris, K. D. Antoniadis, A. A. Mouza, and S. V. Paras, *Int. J. Heat Fluid Flow* 30, 691 (2009).

Received: 9 June 2010. Accepted: 25 January 2011.